Unprecedented Hexa- and Undecanuclear Frameworks of Two New Tin(IV) Oxo Clusters Resulting from Partial Debenzylation Reactions

Laurent Plasseraud, Hélène Cattey, and Philippe Richard

Institut de Chimie Moléculaire de l'Université de Bourgogne (ICMUB), UMR CNRS 5260, UFR Sciences et Techniques, 9 allée A. Savary, BP 47870, 21078 DIJON Cedex, France

Reprint requests to Dr. L. Plasseraud. Fax: +33 (0)3 80 39 60 98.
E-mail: Laurent.Plasseraud@u-bourgogne.fr

Z. Naturforsch. **2010**, *65b,* 1293 – 1300; received June 10, 2010

Dedicated to Professor Georg Süss-Fink on the occasion of his 60th birthday

A new and facile synthetic route to the known neutral cluster $((PhCH_2)_2SnO)_6[((PhCH_2)_2SnOH)_2(CO_3)]_2$ (**2**) as well as its reactivity toward trifluoromethanesulfonic acid (HO_3SCF_3, TfOH) are reported. The solid-state structure of the new solvate $\mathbf{2}\cdot 6C_7H_8$ has been determined by single-crystal X-ray diffraction. The core of **2** can be described as a pair of coplanar pentanuclear $[(PhCH_2)_2SnO]_5$ ladders bridged at their ends by two carbonate groups. Successive additions of TfOH to a suspension of **2** in CD_3CN were monitored by $^{119}Sn\{^1H\}$ NMR spectroscopy showing the transformation of the fingerprint of **2** ($\delta = -244$, -246, -306 ppm), *via* new upfield signals, to a final broad resonance located at $\delta = -474$ ppm. Thereafter, two unprecedented ionic monobenzyltin(IV) oxo clusters, **3** and **4**, resulting from a debenzylation reaction and exhibiting unusual hexa- and undecanuclear frameworks, respectively, have been isolated as single crystals.

Key words: Organotin(IV), Sn-O-Sn Framework, Triflate, Cleavage Reactions, Crystal Structures

Introduction

Organotin compounds with Sn–O bonds have a diversity of solid-state structures, from discrete mononuclear compounds to complex clusters and multidimensional networks. Pioneering work in the field of organotin-oxo clusters is attributable to Holmes and Chandrasekhar who in the 1980's discovered several unexpected polynuclear structures and published the first reviews relating to the classification of these compounds [1]. Since then, the inventory of structures has regularly been updated; it reveals a profuse structural diversity [2]. Indeed, on the basis of X-ray crystallographic studies, a great variety of shapes has already been identified for organotin-oxo derivatives which include prismane [3], butterfly [4], ladder [5], O- and S-capped cluster [6], drum [7], cube [8], double cube [9], football cage [10], crown [11], extended cage [12], and coordination polymer types [13]. Moreover, the structural interrelationship between these polynuclear arrangements has been clearly established, highlighting possible mechanisms of interconversion from one form to another [14]. In the past decade, with the growing interest in the assembly of the metal-organic frameworks (MOFs), organotin-oxo moieties have also been used as building blocks for designing supramolecular architectures with remarkably large cavities [15]. From a synthetic point of view, organotin assemblies containing Sn–O bonds are generally obtained from the reaction of organotin precursors (such as organotin oxides and hydroxides) in the presence of phosphonic, phosphinic, carboxylic, and sulfonic acids at room temperature or under reflux conditions. Recently, reactions with arylarsonic acids were also explored [16]. In numerous examples, the cleavage of Sn–C bonds leads to the formation of Sn–O bonds [17].

Formerly, investigating the direct synthesis of organic carbonates from carbon dioxide and alcohols promoted by organometallic tin(IV) precursors [18], and during recycling experiments, we isolated a deca(organotin(IV)) oxo cluster, characterized as $(n\text{-}Bu_2SnO)_6[(n\text{-}Bu_2SnOCH_3)_2(CO_3)]_2$ and arranged in a pair of coplanar $[(n\text{-}Bu_2Sn)_5O]_5$ ladders bridged by two carbonate groups (Fig. 1) [19].

More recently, we optimized the preparation of this compound by developing a new high-yield route from di-*n*-butyl tin oxide, $n\text{-}Bu_2SnO$, and dimethyl carbonate (DMC) in a sealed vial [20]. Applying the same ex-

0932–0776 / 10 / 1100–1293 $ 06.00

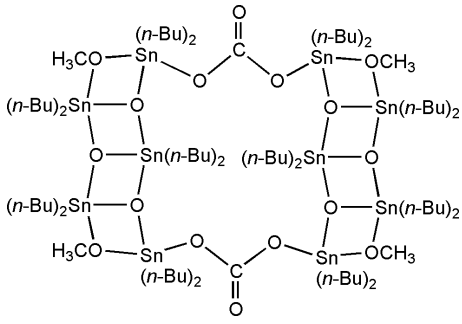

Fig. 1. Molecular representation of $(n\text{-}Bu_2SnO)_6[(n\text{-}Bu_2SnOCH_3)_2(CO_3)]_2$ [19].

perimental protocol, we report herein the synthesis of $((PhCH_2)_2SnO)_6[((PhCH_2)_2SnOH)_2(CO_3)]_2$ (**2**), from $(PhCH_2)_2SnO$ (**1**) used as a tin precursor. The crystal structure of **2**·6C_7H_8(C_7H_8 = free toluene molecules), as determined by single crystal X-ray diffraction, as well as the solution multinuclear NMR characterization are presented. Thereafter, the reactivity of **2** toward four successive additions of trifluoromethanesulfonic acid (TfOH) equivalents was also investigated and monitored by $^{119}Sn\{^1H\}$ NMR spectroscopy in CD_3CN. Two new ionic monobenzyltin(IV) trifluoromethanesulfonate clusters, **3** and **4**, resulting from a debenzylation process have been isolated and characterized by single-crystal X-ray diffraction. To our knowledge, the hexa- and undecanuclear frameworks of **3** and **4**, respectively, are unusual and have never been reported previously in the literature on organotin(IV) oxo clusters.

Results and Discussion

*Synthesis and characterization of $((PhCH_2)_2SnO)_6[((PhCH_2)_2SnOH)_2(CO_3)]_2$ (**2**)*

The reaction of dibenzyltin oxide, $(PhCH_2)_2SnO$ (**1**), with dimethyl carbonate in a sealed vial at 125 °C in the presence of toluene and traces of methanol provides the polynuclear dibenzyltin(IV) oxo cluster, $((PhCH_2)_2SnO)_6[((PhCH_2)_2SnOH)_2(CO_3)]_2$ (**2**). The crystallization of **2** from hot toluene gave rise, upon slow cooling, to air-stable colorless crystals characterized as **2**·6(C_7H_8) by an X-ray crystallographic analysis. In the past, Ma and co-workers reported the isolation of **2**·2CH_3COCH_3, obtained from dibenzyltin dichloride when it was kept in the presence of atmospheric CO_2, with 15 % yield [21]. The synthetic pathway described here involving the use of sealed vial conditions increases the yield significantly up to 44 %.

The $^{119}Sn\{^1H\}$ NMR spectrum in $CDCl_3$ of an analytically pure sample of **2** shows three signals at δ = −243.9, −245.8 and −305.8 ppm (relative intensity 1 : 2 : 2), which is consistent with a pentacoordination of the tin atoms. The $^{13}C\{^1H\}$ NMR spectrum displays at δ = 164.0 ppm the signature of a carbonato ligand, as well as three sets of signals at δ = 30.5, 31.9 and 32.4 ppm assigned to the methylenic groups of benzyl ligands (-CH_2Ph) linked to the three different types of tin atoms of **2**. Interestingly, in the ^1H NMR spectrum, two of the three methylenic groups of benzyl ligands give rise to two AB systems with $^2J_{H\text{-}H}$ = 12.3 and 11.5 Hz. ($^{119}Sn\{^1H\}$, $^{13}C\{^1H\}$ and ^1H NMR spectra of **2** are displayed in the Supporting Information. See note at the end of the paper for availability). The ESI mass spectroscopic analysis (positive mode) exhibited predominant mass clusters at *m/z* = 973 that can be attributed to fragments with three tin atoms, $[(PhCH_2)_2SnO)_3Na]^+$.

Based on an X-ray crystallographic analysis, the inorganic core of **2** can be described as a pair of coplanar pentanuclear $[(PhCH_2)SnO]_5$ ladders bridged at their ends by two carbonate groups acting as μ_1,μ_1-bridging ligands and stabilized by four μ_2-bridging hydroxy groups. An ORTEP view of the molecular structure of **2**, and selected bond lengths and angles are available in the Supporting Information. In addition, six molecules of toluene co-crystallize in the crystal lattice with **2** and are regularly intercalated between organotin frameworks leading to the formation of a channel-like organisation (Fig. 2). From a structural point of view, the double coplanar ladder-type structure constitutes a remarkable feature, up to now exclusively

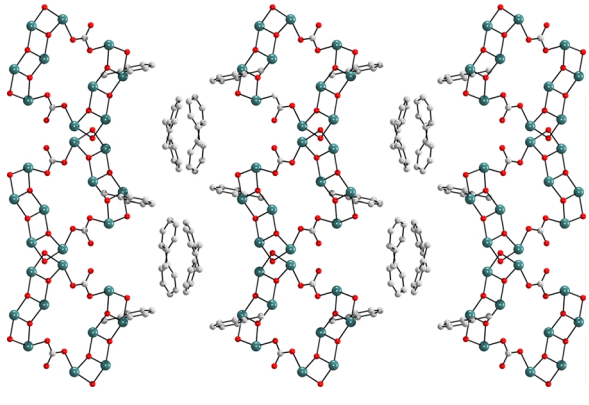

Fig. 2 (color online). DIAMOND view showing the intercalation of toluene molecules between macrocyclic frameworks of **2** (hydrogen atoms and benzyl ligands are omitted for clarity; Sn blue, O red, C grey).

observed in the case of di-*n*-butyl- and dibenzyltin oxo clusters [19, 21, 22].

*Reactivity of $((PhCH_2)_2SnO)_6[((PhCH_2)_2SnOH)_2(CO_3)]_2$ (**2**) toward trifluoromethanesulfonic acid (TfOH)*

Numerous examples of trifluoromethanesulfonate derivatives have been reported previously in organotin(IV) chemistry and structurally characterized by single-crystal X-ray diffraction [23]. In general, organotin triflates are obtained by reaction of organotin oxides with HO_3SCF_3 (TfOH) or alternatively from organotin chlorides ($R_{(4-x)}SnCl_x$) and AgO_3SCF_3. In the past using the second synthetic approach, we have described the solid-state structure of the *catena*-poly[[di-*n*-butyltin(IV)]-μ-trifluoromethanesulfonato-[[di-*n*-butyl(trifluoromethanesulfonato)-di-μ-hydroxotin(IV)]] with bridging as well as terminal trifluoromethanesulfonate ligands [24]. Recently, continuing our investigation in this domain, we published the preparation of an unexpected trifluoromethanesulfonato di-*n*-butylin(IV)-based supramolecular 2D framework induced by phenazine [15f]. In addition to the structural interest, organotin(IV) trifluoromethanesulfonate complexes are active in homogeneous catalysis as Lewis acids for organic reactions such as the Mukaiyama aldol reaction [25], the Robinson annulation [26], the acetylation of alcohols [27], and the transesterification of dimethyl carbonate with phenol [28].

The addition of trifluoromethanesulfonic acid to a suspension of **2** in acetonitrile gave a clear solution after stirring for 2 h at r. t. Removal of solvent *in vacuo* and washing of the tin-based residue with dichloromethane yielded a homogeneous colorless powder. Interestingly, the $^{119}Sn\{^1H\}$ NMR spectrum of the powder dissolved in CD_3CN shows an upfield signal located at $\delta = -474.2$ ppm suggesting the presence of hexacoordinated tin atoms. In the $^{13}C\{^1H\}$ and $^{19}F\{^1H\}$ NMR spectra the coupling constant of 318 Hz between the ^{13}C and ^{19}F nuclei, with $\delta(^{13}C) = 121.05$ and $\delta(^{19}F) = -79.05$ ppm, can be attributed to CF_3 moieties. The electrospray mass spectrum (positive mode) displays six intense mass clusters at *m/z* = 953, 965, 1025, 1041, 1100, and 1115, not assigned precisely but exhibiting assuredly characteristic isotope distribution patterns of polynuclear tin species. The IR spectrum of the colorless showed a very broad absorption centered at 3396 cm^{-1} as well as a sharp band at 3596 cm^{-1} which can be attributed

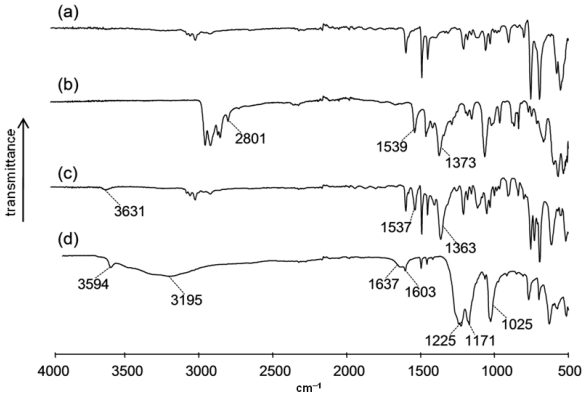

Fig. 3. IR(ATR) spectra of (a) $(PhCH_2)_2SnO$ (**1**), (b) $(n\text{-}Bu_2SnO)_6[(n\text{-}Bu_2SnOCH_3)_2(CO_3)]_2$, (c) $((PhCH_2)_2SnO)_6[((PhCH_2)_2SnOH)_2(CO_3)]_2$ (**2**), and (d) fingerprint of the tin-based powder resulting from the addition of TfOH to **2** in acetonitrile.

to the presence of hydroxyl groups. Characteristic vibrational bands of trifluoromethanesulfonate ligands, in particular $\nu(CF_3)$ and $\nu(SO_3)$, are also observed in the region between 1000 and 1300 cm^{-1} (Fig. 3d) [29].

In order to confirm the spectroscopic observations, we attempted to crystallize the tin compounds to gain structural data. Dissolving the colorless powder in a mixture of acetonitrile/dichloromethane/toluene, after several days we got two types of colorless single crystals. However, owing to the morphologic resemblance of the crystals, the selective collection was difficult. Both compounds, hereinafter referred to **3** and **4**, have two distinct molecular structures which are reported and discussed in the next sections.

In parallel with structural investigations we reproduced the experiment under NMR tube conditions in CD_3CN, monitoring the *in situ* reactivity of **2** with trifluoromethanesulfonic acid at r. t. We collected the $^{119}Sn\{^1H\}$ NMR spectra of the mixture after successive additions of a total of four molar equivalents of TfOH (Fig. 4). After the first addition of TfOH the spectrum shows clearly that the initial fingerprint of **2** was modified displaying three new peaks at $\delta = -217.1$, -243.0 and -292.9 ppm (Fig. 4b). Two additional aliquots of TfOH led to several unknown signals, first located at $\delta = -220.5$, -245.2, -253.0, -293.9, and -516.4 ppm (Fig. 4c), and then at $\delta = -294.9$ and -472.5 ppm (Fig. 4d). Finally, the last addition of TfOH gave only one broad upfield resonance at $\delta = -472.4$ ppm (Fig. 4e) that is comparable to the chemical shift directly saved from the colorless powder obtained during the initial reaction in a Schlenk

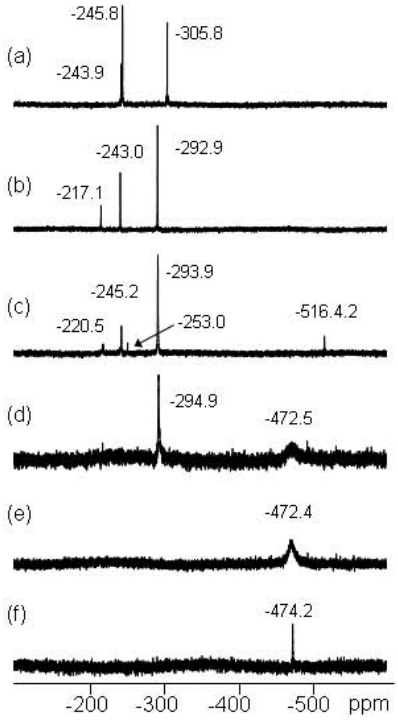

Fig. 4. $^{119}Sn\{^1H\}$ NMR spectra of (a) $((PhCH_2)_2SnO)_6$-$[((PhCH_2)_2SnOH)_2(CO_3)]_2$ (**2**) in $CDCl_3$, (b, c, d, e) successive additions of a total of 4 equivalents of TfOH to a suspension of **2** in CD_3CN, and (f) powder precursor of **3** and **4** in CD_3CN.

tube (Fig. 4f), and which suggests an increase of the coordination number of the tin atoms from five to six.

*Molecular structure of $[(C_7H_7Sn)_6(\mu_4\text{-}O)(\mu\text{-}OH)_{11}(H_2O)_4](OTf)_5$ (**3**)*

The solid-state structure of **3** consists of a hexanuclear cation bearing five positive charges, surrounded by five uncoordinated trifluoromethanesulfonate anions and solvate water molecules. An ORTEP view of the cation is shown in Fig. 5. Selected bond lengths and angles are available in the Supporting Information. All tin atoms of **3** are hexacoordinated with distorted octahedral geometry and are bound to only one benzyl ligand in a η^1 mode. However, their chemical environment differs, and we can distinguish two crystallographically distinct types of tin atoms. The Sn1 and Sn6 sites are each coordinated to two molecules of water and to three bridging OH groups while Sn2, Sn3, Sn4 and Sn5 are all connected to a μ_4 oxygen atom as well as to four μ-OH groups.

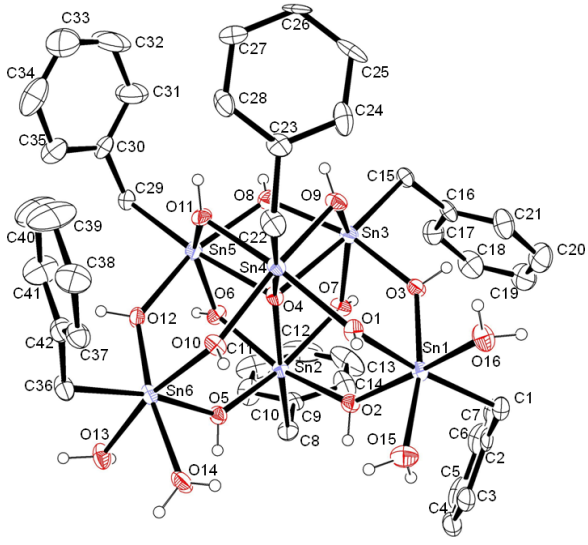

Fig. 5 (color online). ORTEP view of the molecular structure of $[(C_7H_7Sn)_6(\mu_4\text{-}O)(\mu\text{-}OH)_{11}(H_2O)_4](OTf)_5$ (**3**) with the crystallographic numbering scheme (hydrogen atoms, except for OH groups, counter anions and solvent molecules are omitted for clarity; Sn blue, O red, C white).

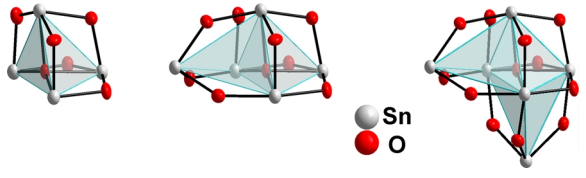

Fig. 6 (color online). Reconstitution of the inorganic framework of **3**, highlighting the arrangement of a bicapped tetrahedron architecture (DIAMOND representation).

Interestingly, taking into consideration the polyhedra described by the tin atoms, the construction of **3** can be viewed as a bicapped tetrahedron architecture. Indeed, the Sn2, Sn3, Sn4 and Sn5 sites constitute the vertices of the central tetrahedron and two of the four faces, defined by Sn2-Sn3-Sn4 and Sn2-Sn4-Sn5, are capped by the Sn1 and Sn6 atoms, respectively, giving rise to the unprecedented hexanuclear core of **3**. A DIAMOND representation detailing the reconstitution of the framework of **3** is depicted in Fig. 6.

In the past, similar architectures, then described as a bicapped tetrahedron or a "chain" of three tetrahedra sharing faces, were observed in particular for hexanuclear clusters of lead and osmium (β-$[Pb_6O(OH)_6^{4+}]$ [30], $Os_6(CO)_{18}$ [31]). To the best of our knowledge, compound **3** constitutes the first example for organotin(IV) complexes presenting such a structure.

*Molecular structure of {Sn(μ-OH)$_6$[(C$_7$H$_7$Sn)$_{10}$-(μ$_4$-O)$_2$(μ-OH)$_{16}$(H$_2$O)$_2$(OTf)$_2$]}(OTf)$_6$ (**4**)*

The solid-state structure of **4** consists of a centrosymmetric undecanuclear cation bearing six positive charges, which is surrounded by six uncoordinated trifluoromethanesulfonate anions and two dichloromethane solvate molecules. An ORTEP view of the cation is shown in Fig. 7. Selected bond lengths and angles are available in the Supporting Information. All tin atoms of **4** are hexacoordinated with distorted octahedral geometry, but three crystallographically distinct tin sites can be recognized. The Sn1 site, located at the center of inversion, is occupied by a tin atom connected to six bridging OH groups, which was generated by a complete debenzylation. The Sn6 and Sn6^i atoms are each coordinated to one molecule of water [Sn–O(H)$_2$ = 2.198(7) Å], to one terminal trifluoromethanesulfonato ligand in an η^1 mode [Sn–O(Tf) = 2.229(7) Å] and to three bridging OH groups, while Sn2, Sn2^i, Sn3, Sn3^i, Sn4, Sn4^i, Sn5, and Sn5^i are all connected to one of the two central μ_4 oxygen atoms as well as to four μ-OH groups. With the exception of Sn1, all tin atoms are bound to one benzyl ligand. The framework of **4** can be considered as two pentanuclear moieties, Sn$_5$O$_9$, bound together by a dealkylated tin atom, and through six bridging OH groups. Few crystal structure determinations of polyhydroxyorganotin clusters exhibiting remarkable decanuclear ([(2,4,6-^{i}Pr$_3$C$_6$H$_2$Sn)$_7$Sn$_3$(4-MeC$_6$H$_4$SO$_3$)$_2$(μ$_2$-OH)$_{16}$(OH)$_3$-(OH)$_3$(μ$_3$-O)$_3$(μ$_4$-OH)][(4-MeC$_6$H$_4$SO$_3$)]$_4$ [32]) and dodecanuclear skeletons ([(2,4,6-^{i}Pr$_3$C$_6$H$_2$Sn)$_8$-(μ$_4$-O)$_2$(μ$_3$-O)$_8$(μ$_2$-O)$_4$(μ$_2$-OH)$_8${Sn(OH)}$_4$] [33], {(BuSn)$_{12}$O$_{14}$(OH)$_6$}(O$_2$PPh$_2$)$_2$ [34], {(BuSn)$_{12}$O$_{14}$-(OH)$_6$}(4-CH$_3$C$_6$H$_4$SO$_3$)$_2$ [35] and Sn$_{12}$O$_8$(OH)$_4$-(OEt)$_{28}$(HOEt)$_4$ [36]) have been previously published by the groups of Jousseaume and Ribot, respectively. To our knowledge, the undecanuclear structure of **4** is unusual and constitutes the first example of an Sn$_{11}$ edifice reported until now.

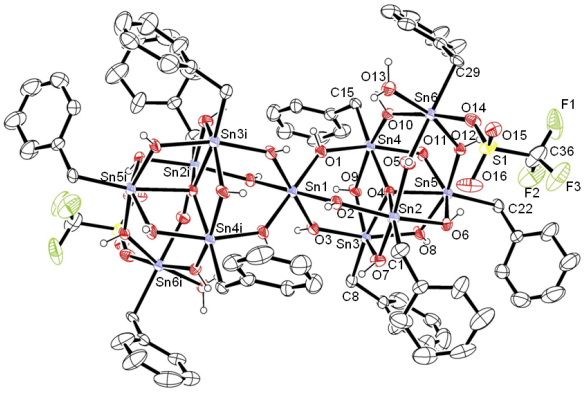

Fig. 7 (color online). ORTEP view of the molecular structure of {Sn(μ-OH)$_6$[(C$_7$H$_7$Sn)$_{10}$(μ$_4$-O)$_2$(μ-OH)$_{16}$(H$_2$O)$_2$-(OTf)$_2$]}(OTf)$_6$ (**4**) with the crystallographic numbering scheme (hydrogen atoms, except for OH groups, counter anions and solvent molecules are omitted for clarity; Sn blue, O red, C white, S yellow, F green).

Conclusion

In summary, this work has opened a route giving satisfactory yields of the decanuclear cluster ((PhCH$_2$)$_2$-SnO)$_6$[((PhCH$_2$)$_2$SnOH)$_2$(CO$_3$)]$_2$ (**2**) demonstrating the relevance of the synthetic method carried out under sealed vial conditions. The reactivity of **2** toward trifluoromethanesulfonic acid was investigated. In presence of a large excess of HO$_3$SCF$_3$, the organotin oxo cluster **2** undergoes a debenzylation reaction leading to the formation of hexa- and undecanuclear architectures, characterized by X-ray crystallographic analysis as [(C$_7$H$_7$Sn)$_6$(μ$_4$-O)(μ-OH)$_{11}$-(H$_2$O)$_4$](OTf)$_5$ (**3**) and {Sn(μ-OH)$_6$[(C$_7$H$_7$Sn)$_{10}$(μ$_4$-O)$_2$(μ-OH)$_{16}$(H$_2$O)$_2$(OTf)$_2$]}(OTf)$_6$ (**4**). The Sn$_6$ and Sn$_{11}$ cores are unprecedented and thus expand further the extraordinary diversity of organotin(IV) oxo clusters. In addition, the *in situ* ^{119}Sn{^{1}H} NMR experiments with TfOH have shown non-identified resonances, suggesting the formation of additional tin-based intermediates. Further investigations are in progress in our laboratory in an attempt to elucidate their solid-state structures.

Experimental Section

All manipulations were carried out by using standard Schlenk techniques [37] or sealed reaction vessels. The organic solvents were refluxed over appropriate desiccants, distilled and saturated with argon prior to use. Chemicals were purchased from Aldrich and Acros Organics. The starting compound (PhCH$_2$)$_2$SnCl$_2$ was synthesized from tin according to a published method [38]. The standard NMR spectra were recorded in CDCl$_3$ and CD$_3$CN on Bruker Avance 300 and II 600 spectrometers. ^{1}H and ^{13}C chemical shifts (δ, ppm) were determined from the residual solvent signal (*C*H*C*l$_3$ δ = 7.24, *C*DCl$_3$ δ = 77.00). ^{119}Sn{^{1}H} and ^{19}F chemical shifts (δ, ppm) are reported downfield from (CH$_3$)$_4$Sn and trifluoromethylbenzene, respectively, used as internal standards. IR spectra were recorded on a Bruker Vector 22 instrument with a Specac Golden Gate™ ATR device. The ESI mass spectrum was obtained on a Bruker

Table 1. Crystal and structure refinement data for **2**, **3** and **4**.

Compounds	**2**	**3**	**4**
Empirical formula	$C_{142}H_{144}O_{16}Sn_{10}$ $\cdot 6(C_7H_8)$	$C_{42}H_{61}O_{16}Sn_6$ $\cdot 5(CF_3SO_3)\cdot 5(H_2O)$	$C_{72}H_{96}F_6O_{32}S_2Sn_{11}$ $\cdot 6(CF_3SO_3)\cdot 2(CH_2Cl_2)$
Formula weight, g mol^{-1}	3846.28	2369.60	4021.72
Crystal size, mm^3	0.25 × 0.17 × 0.17	0.10 × 0.05 × 0.05	0.20 × 0.05 × 0.05
Temperature, K	115(2)	115(2)	115(2)
Crystal system	orthorhombic	triclinic	triclinic
Space group	*P*bca	$P\bar{1}$	$P\bar{1}$
a, Å	21.4820(2)	14.0503(3)	15.3872(4)
b, Å	19.3639(1)	16.3481(3)	15.4895(3)
c, Å	39.8992(3)	17.7866(4)	16.7265(5)
α, deg	90	103.887(1)	116.275(1)
β, deg	90	93.839(1)	102.399(1)
γ, deg	90	91.128(1)	105.211(2)
Volume, Å^3	16597.1(2)	3954.49(14)	3187.31(14)
Z	4	2	1
ρ_{calc}, g cm^{-3}	1.54	1.98	2.09
μ, mm^{-1}	1.5	2.1	2.4
F(000)	7696	2292	1942
$((\sin\theta)/\lambda)_{max}$, Å^{-1}	0.65	0.65	0.65
Index ranges *hkl*	*h*: −27; 27	*h*: −18; 18	*h*: −19; 19
	k: −25; 25	*k*: −17; 21	*k*: −20; 20
	l: −51; 51	*l*: −23; 21	*l*: −21; 20
Refl. coll. / unique / R_{int}	34530 / 18670 / 0.0518	29840 / 17946 / 0.0786	26361 / 14565 / 0.0808
Reflections with $I \geq 2\sigma(I)$	12620	9590	7607
Data / restr. / ref. param.	18670 / 2 / 877	17946 / 104 / 1109	14565 / 36 / 849
Final *R*1 / *wR*2 [$I \geq 2\sigma(I)$][a, b]	0.0415 / 0.0654	0.0606 / 0.1141	0.0722 / 0.1582
Final *R*1 / *wR*2 (all data)[a, b]	0.0864 / 0.0730	0.1484 / 0.1399	0.1589 / 0.1930
A / B (weighting scheme)[b]	0.0135 / 28.8302	0.0540 / 0	0.0922 / 0
Goodness-of-fit[c] on F^2	1.052	0.988	1.027
Largest difference peak / hole, e Å^{-3}	0.58 / −0.75	2.04 / −1.27	1.85 / −1.12
CCDC deposition no.	763719	763718	763717

[a] $R1 = \Sigma||F_o| - |F_c||/\Sigma|F_o|$; [b] $wR2 = [\Sigma w(F_o^2 - F_c^2)^2/\Sigma w(F_o^2)^2]^{1/2}$, $w = [\sigma^2(F_o^2)+(AP)^2+BP]^{-1}$, where $P = (\mathrm{Max}(F_o^2, 0)+2F_c^2)/3$ and A and B are constants adjusted by the program; [c] GoF = $S = [\Sigma w(F_o^2 - F_c^2)^2/(n_{obs} - n_{param})]^{1/2}$, where n_{obs} is the number of data and n_{param} the number of refined parameters.

microOTOF-Q instrument using a methanol mobile phase. Elemental analyses were performed at the Institut de Chimie Moléculaire, Université de Bourgogne, Dijon.

*Synthesis of $(PhCH_2)_2SnO$ (**1**)*

A solution of KOH (2.237 g, 0.056 mol) in water (7 mL) was added dropwise to a solution of $(PhCH_2)SnCl_2$ (9.763 g, 0.026 mol) in acetone (65 mL). The mixture was stirred for 2 h at r. t., and then the resultant colorless precipitate was filtered off, washed with acetone, and dried under vacuum. Yield: 7.062 g (86 %). – IR: ν = 3078w, 3057w, 3022m, 2921w, 1598s, 1491vs, 1450s, 1208m, 1059 m, 1029m, 904m, 754vs, 694vs, 578s, 552vs cm^{-1}. – $C_{14}H_{14}OSn$ (316.97): calcd. C 53.05, H 4.45; found C 53.66, H 4.42.

*Synthesis of $((PhCH_2)_2SnO)_6[((PhCH_2)_2SnOH)_2(CO_3)]_2$ (**2**)*

A mixture of $(PhCH_2)_2SnO$ (**1**) (1.116 g, 3.523 mmol), dimethyl carbonate (0.5 mL) and methanol (0.5 mL) in toluene (25 mL) was heated in a sealed vial at 398 K. After *ca*. 30 min, the suspension turned to a turbid solution, and heating was continued for 50 min. After cooling down to r. t., filtration and removal of the volatiles under vacuum, a colorless solid was obtained. Crystallization of the residue from hot toluene (15 mL) led, after cooling to room temperature, to air-stable crystals which were characterized as the title compound. Yield: 0.515 g (44 % based on crystalline material). – ^{1}H NMR (600.130, 298 K, $CDCl_3$): δ = 1.22 (s, O*H*, 4H), 2.07 and 2.31 (*AB* system, 2 × $^2J_{H\text{-}H}$ = 12.3 Hz, 2 × -SnCH*H′*Ph, 2 × 8H), 2.66 and 3.04 (*AB* system, 2 × $^2J_{H\text{-}H}$ = 11.5 Hz, 2 × -C*H*H′Ph, 2 × 8H), 3.29 (s, $^2J^1$H-$^{117/119}$Sn = 92.9 Hz, -CH_2Ph, 8H), 6.40 – 7.50 (m, -CH$_2$*Ph*, 100H). – ^{13}C{^{1}H} NMR (75.467 MHz, 300 K, $CDCl_3$): δ = 164.0 (-SnOC(O)OSn-), 140.6 (-SnCH$_2$*Ph*), 139.2 (-SnCH$_2$*Ph*), 138.6 (-SnCH$_2$*Ph*), 128.8 (-SnCH$_2$*Ph*), 128.4 (-SnCH$_2$*Ph*), 128.2 (-SnCH$_2$*Ph*), 127.9 (-SnCH$_2$*Ph*), 127.6 (-SnCH$_2$*Ph*), 127.2 (-SnCH$_2$*Ph*), 124.7 (-SnCH$_2$*Ph*), 124.6 (-SnCH$_2$*Ph*), 124.4 (-SnCH$_2$*Ph*), 32.4 (-Sn*C*H$_2$Ph), 31.9 (-Sn*C*H$_2$Ph), 30.5 (-Sn*C*H$_2$Ph). –

$^{119}Sn\{^1H\}$ NMR (111.920 MHz, 297 K, $CDCl_3$): δ = −243.9 (2Sn), −245.8 (4Sn), −305.8 (4Sn). – IR: ν = 3631w, 3080w, 3058w, 3024m, 2921w, 1599m, 1537m, 1491s, 1451m, 1363s, 1209m, 1113m, 1051m, 1030m, 908m, 754vs, 730s, 693vs, 614s, 516s cm^{-1}. – MS ((+)-ESI): *m/z* = 973 $[(PhCH_2)_2SnO)_3Na]^+$. – $C_{142}H_{144}O_{16}Sn_{10}$ (3293.59): calcd. C 51.78; H 4.42; found C 51.85; H 5.08.

*Isolation of clusters **3** and **4***

Triflic acid (55 μL, 0.624 mmol) was added to $((PhCH_2)_2SnO)_6[((PhCH_2)_2SnOH)_2(CO_3)]_2$ (**2**) (0.130 g, 0.039 mmol) suspended in acetonitrile (5 mL) and stirred at r. t. After 2 h, a clear solution resulted, and filtration followed by evaporation afforded crude products which were washed with CH_2Cl_2 to furnish a colorless powder (yield: 0.089 g). The powder residue was then crystallized from a mixture of acetonitrile-dichloromethane-toluene, at r. t., giving after several days two types of single crystals suitable for X-ray crystallographic studies, which were characterized as compounds **3** and **4**, respectively.

X-Ray structure determinations

Diffraction data were collected from suitable crystals on a Nonius Kappa CCD diffractometer (MoK_α radiation, λ = 0.71073 Å) at 115 K. The structures of **2**, **3** and **4** were solved using Direct Methods (SIR 92) [39] and refined with full-matrix least-squares methods based on F^2 (SHELXL-97) [40] with the aid of the WINGX program [41]. Except for atoms belonging to some disordered groups, all non-hydrogen atoms were refined with anisotropic thermal parameters. Hydrogen atoms attached to carbon atoms were included in their calculated positions and refined with a riding model, while the coordinates of the hydrogen atoms bonded to oxygen atoms were refined with a set of restraints. For compound **3**, one of the phenyl groups was found disordered over two positions with occupation factors converging to 0.54 : 0.46. Two triflate counter ions were also found disordered with occupation factors 0.71 : 0.29 and 0.65 : 0.35, respectively. The minor components of theses disordered groups were isotropically refined with restraints applied on the C–F, F–F, S–O and O–O distances. Furthermore, five water molecules were located in the asymmetric unit of which one was found disordered over two positions with occupancy factors 0.64 : 0.36. Hydrogen atoms of these solvent molecules were not located. Crystallographic data and structure refinement details for compounds **2**–**4** are listed in Table 1. Selected bond lengths and angles for compounds **2**, **3** and **4** are given as Supporting Information (Tables S1 – S3, respectively). Programs used for the representation of the molecular and crystal structures: ORTEP [42], DIAMOND [43].

CCDC 763717–763719 contain the supplementary crystallographic data for this paper. These data can be obtained free of charge from The Cambridge Crystallographic Data Centre *via* www.ccdc.cam.ac.uk/data_request/cif.

Supporting Information

The ^1H, $^{13}C\{^1H\}$, $^{119}Sn\{^1H\}$ NMR spectra, and an ORTEP view of the molecular structure of **2** are shown in the Supporting Information (Figs. S1 – S4, respectively), selected bond lengths and angles for compounds **2**, **3** and **4** are given in Tables S1 – S3. This material is available online only.

Acknowledgements

We gratefully acknowledge the Centre National de la Recherche Scientifique (CNRS, France) and the Agence Nationale de la Recherche (ANR-08-CP2D-18, France) for supports of this work. L. P. wishes to thank in particular Dr. S. Chambrey (sample of $(PhCH_2)_2SnO$), Dr. B. Hanquet (NMR experiments), Ms. M.-J. Penouilh (ES-MS measurements), Mr. M. Soustelle (elemental analyses) as well as Mr. P. Yapp (correction of the manuscript in English).

[1] a) R. R. Holmes, *Acc. Chem. Res*. **1989**, *22*, 190 – 197; b) R. R. Holmes, R. O. Day, K. C. Kumara Swamy, C. G. Schmid, S. D. Burton, J. M. Holmes, *Main Group Metal Chemistry* **1989**, *12*, 291 – 303.

[2] a) R. R. Holmes, *Phosphorus, Sulfur, Silicon, Relat. Elem*. **1999**, *150*, 1 – 40; b) V. Chandrasekhar, S. Nagendran, V. Baskar, *Coord. Chem. Rev*. **2002**, *235*, 1 – 52.

[3] K. C. Kumara Swamy, M. A. Said, S. Nagabrahmanandachari, D. M. Poojary, A. Clearfield, *J. Chem. Soc., Dalton Trans*. **1998**, 1645 – 1651.

[4] R. R. Holmes, K. C. Kumara Swamy, C. G. Schmid, R. O. Day, *J. Am. Chem. Soc*. **1988**, *110*, 7060 – 7066.

[5] J. Beckmann, D. Dakternieks, A. Duthie, F. S. Kuan, E. R. T. Tiekink, *Organometallics* **2003**, *22*, 4399 – 4404.

[6] C. G. Schmid, R. O. Day, R. R. Holmes, *Phosphorus, Sulfur, Silicon, Relat. Elem*. **1989**, *41*, 69 – 74.

[7] V. Chandrasekhar, R. O. Day, R. R. Holmes, *Inorg. Chem*. **1985**, *24*, 1970 – 1971.

[8] K. C. Kumara Swamy, R. O. Day, R. R. Holmes, *J. Am. Chem. Soc*. **1987**, *109*, 5546 – 5548.

[9] K. C. Kumara Swamy, R. O. Day, R. R. Holmes, *J. Am. Chem. Soc*. **1988**, *110*, 7543 – 7544.

[10] F. Banse, F. Ribot, P. Tolédano, J. Maquet, C. Sanchez, *Inorg. Chem*. **1995**, *34*, 6371 – 6379.

[11] K. C. Kumara Swamy, C. G. Schmid, R. O. Day, R. R. Holmes, *J. Am. Chem. Soc*. **1988**, *110*, 7067 – 7076.

[12] V. Chandrasekhar, V. Baskar, A. Steiner, S. Zacchini, *Organometallics* **2002**, *21*, 4528 – 4532.

[13] S.-Y. Song, J.-F. Ma, J. Yang, L.-L. Gao, Z.-M. Su, *Organometallics* **2007**, *26*, 2125 – 2128.

[14] V. Chandrasekhar, K. Gopal, P. Thilagar, *Acc. Chem. Res*. **2007**, *40*, 420 – 434.

[15] a) S. P. Narula, S. Kaur, R. Shankar, S. Verma, P. Venugopalan, S. K. Sharma, *Inorg. Chem*. **1999**, *38*, 4777 – 4783; b) R. García-Zarracino, J. Ramos-Quiñones, H. Höpfl, *Inorg. Chem*. **2003**, *42*, 3835 – 3845; c) R. García-Zarracino, H. Höpfl, *J. Am. Chem. Soc*. **2005**, *127*, 3120 – 3130; d) V. Chandrasekhar, R. Thirumoorthi, R. Azhakar, *Organometallics* **2007**, *26*, 26 – 29; e) R. García-Zarracino, H. Höpfl, M. Güizado-Rodriguez, *Cryst. Growth Des*. **2009**, *9*, 1651 – 1654; f) L. Plasseraud, H. Cattey, P. Richard, D. Ballivet-Tkatchenko, *J. Organomet. Chem*. **2009**, *694*, 2386 – 2394.

[16] Y.-P. Xie, J. Yang, J.-F. Ma, L.-P. Ma, L.-P. Zhang, S.-Y. Song, Z.-M. Su, *Chem. Eur. J*. **2008**, *14*, 4093 – 4103.

[17] For a recent review see: V. Chandrasekhar, K. Gopal, P. Sasikumar, R. Thirumoorthi, *Coor. Chem. Rev*. **2005**, *249*, 1745 – 1765.

[18] a) D. Ballivet-Tkatchenko, O. Douteau, S. Stutzmann, *Organometallics* **2000**, *19*, 4563 – 4567; b) D. Ballivet-Tkatchenko, T. Jerphagnon, R. Ligabue, L. Plasseraud, D. Poinsot, *Appl. Catal. A: General* **2003**, *255*, 93 – 99; c) D. Ballivet-Tkatchenko, H. Chermette, L. Plasseraud, O. Walter, *Dalton Trans*. **2006**, 5167 – 5175; d) D. Ballivet-Tkatchenko, R. Burgat, S. Chambrey, L. Plasseraud, P. Richard, *J. Organomet. Chem*. **2006**, *691*, 1498 – 1504; e) L. Plasseraud, H. Cattey, P. Richard, *Z. Naturforsch*. **2009**, *64b*, 831 – 834.

[19] D. Ballivet-Tkatchenko, S. Chambrey, R. Keiski, R. A. Ligabue, L. Plasseraud, P. Richard, H. Turunen, *Catal. Today* **2006**, *115*, 80 – 87.

[20] L. Plasseraud, D. Ballivet-Tkatchenko, H. Cattey, S. Chambrey, R. Ligabue, P. Richard, R. Willem, M. Biesemans, *J. Organomet. Chem*. **2010**, *695*, 1618 – 1626.

[21] G.-L. Zheng, J.-F. Ma, J. Yang, Y.-Y. Li, X.-R. Hao, *Chem. Eur. J*. **2004**, *10*, 3761 – 3768.

[22] C. Ma, J. Zhang, Q. Jiang, R. Zhang, *Inorg. Chim. Acta* **2004**, *357*, 2791 – 2797.

[23] J. Beckmann, *Appl. Organomet. Chem*. **2005**, *19*, 494 – 499.

[24] D. Ballivet-Tkatchenko, H. Cattey, L. Plasseraud, P. Richard, *Acta Crystallogr.* **2006**, *E62*, m2820 – m2822.

[25] T. Sato, Y. Wakahara, J. Otera, H. Nozaki, *Tetrahedron* **1991**, *47*, 9773 – 9782.

[26] T. Sato, Y. Wakahara, J. Otera, H. Nozaki, *Tetrahedron Lett*. **1990**, *31*, 1581 – 1584.

[27] K. Sakamoto, Y. Hamada, H. Akashi, A. Orita, J. Otera, *Organometallics* **1999**, *18*, 3555 – 3557.

[28] H. Lee, J. Y. Bae, O. S. Kwon, S. J. Kim, S. D. Lee, H. S. Kim, *J. Organomet. Chem*. **2004**, *689*, 1816 – 1820.

[29] a) G. A. Lawrance, *Chem. Rev*. **1986**, *86*, 17 – 33; b) D. H. Johnston, D. F. Shriver, *Inorg. Chem*. **1993**, *32*, 1045 – 1047.

[30] Å. Olin, R. Söderquist, *Acta. Chem. Scand*. **1972**, *26*, 3505 – 3514.

[31] C. Zheng, R. Hoffmann, D. R. Nelson, *J. Am. Chem. Soc*. **1990**, *112*, 3784 – 3791.

[32] G. Prabusankar, B. Jousseaume, T. Toupance, H. Allouchi, *Dalton Trans*. **2007**, 3121 – 3123.

[33] G. Prabusankar, B. Jousseaume, T. Toupance, H. Allouchi, *Angew. Chem.* **2006**, *118*, 1277 – 1280; *Angew. Chem. Int. Ed*. **2006**, *45*, 1255 – 1258.

[34] F. Ribot, C. Sanchez, R. Willem, J. C. Martins, M. Biesemans, *Inorg. Chem*. **1998**, *37*, 911 – 917.

[35] C. Eychenne-Baron, F. Ribot, N. Steunou, C. Sanchez, *Organometallics* **2000**, *19*, 1940 – 1949.

[36] F. Ribot, E. Martnez-Ferrero, K. Boubekeur, P. M. S. Hendrickx, J. C. Martins, L. Van Lokeren, R. Willem, M. Biesemans, *Inorg. Chem*. **2008**, *47*, 5831 – 5840.

[37] D. F. Shriver, M. A. Drezdzon, *The Manipulation of Air-Sensitive Compounds*, 2nd ed., J. Wiley and Sons, New York, **1986**.

[38] K. Sisido, Y. Takeda, Z. Kinugawa, *J. Am. Chem. Soc*. **1961**, *83*, 538 – 541.

[39] A. Altomare, G. Cascarano, C. Giacovazzo, A. Guagliardi, SIR92, A Program for the Automatic Solution of Crystal Structures by Direct Methods. See also: *J. Appl. Crystallogr*. **1993**, *26*, 343 – 350.

[40] G. M. Sheldrick, SHELX-97 (includes SHELXS-97 and SHELXL-97; release 97-2), Program for Crystal Structure Determination, University of Göttingen, Göttingen (Germany) **1998**. See also: G. M. Sheldrick, *Acta Crystallogr.* **1990**, *A46*, 467 – 473; *ibid.* **2008**, *A64*, 112 – 122.

[41] L. J. Farrugia, WINGX, A MS-Windows System of Programs for Solving, Refining and Analysing Single X-Ray Diffraction Data of Small Molecules, University of Glasgow, Glasgow, Scotland (U. K.) **2005**. See also: L. J. Farrugia, *J. Appl. Crystallogr*. **1999**, *32*, 837 – 838.

[42] C. K. Johnson, M. N. Burnett, ORTEP-III, Rep. ORNL-6895, Oak Ridge National Laboratory, Oak Ridge, TN (USA) **1996**. Windows version: L. J. Farrugia, University of Glasgow, Glasgow, Scotland (U. K.) **1999**. See also: L. J. Farrugia, *J. Appl. Crystallogr.* **1997**, *30*, 565.

[43] K. Brandenburg, DIAMOND (version 3.1), Crystal and Molecular Structure Visualization, Crystal Impact – K. Brandenburg & H. Putz GbR, Bonn (Germany) **2005**.

Unprecendented Hexa- and Undecanuclear Frameworks of Two New Tin(IV)-Oxo Clusters Resulting from Partial Debenzylation Reactions

Laurent Plasseraud*, Hélène Cattey, and Philippe Richard

Institut de Chimie Moléculaire de l'Université de Bourgogne (ICMUB),
UMR CNRS 5260, UFR Sciences et Techniques, 9 allée A. Savary, BP 47870,
F-21078 DIJON Cedex, France

Supporting Information

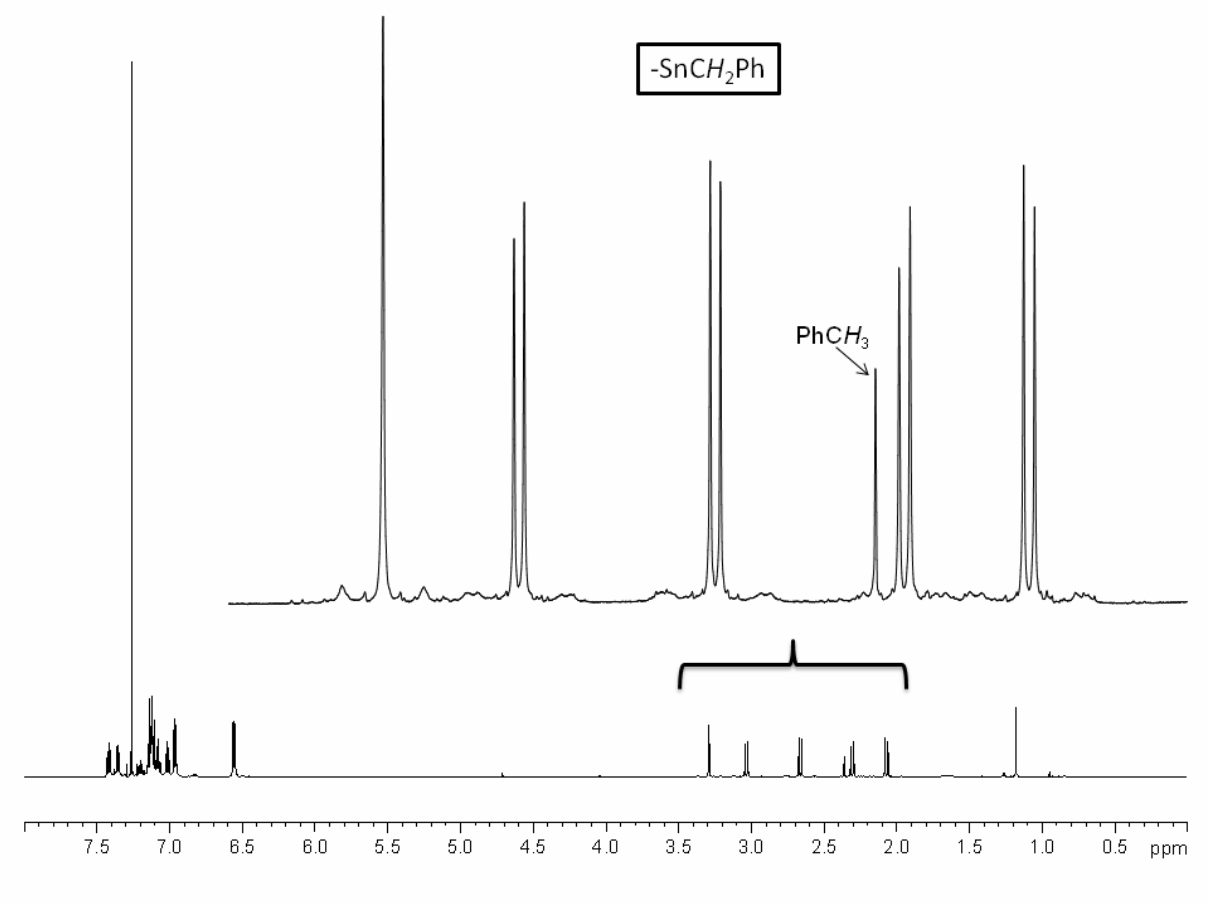

Fig. S1. ^{1}H NMR Spectrum of **2** ($CDCl_3$, 298 K, 600.130 MHz)

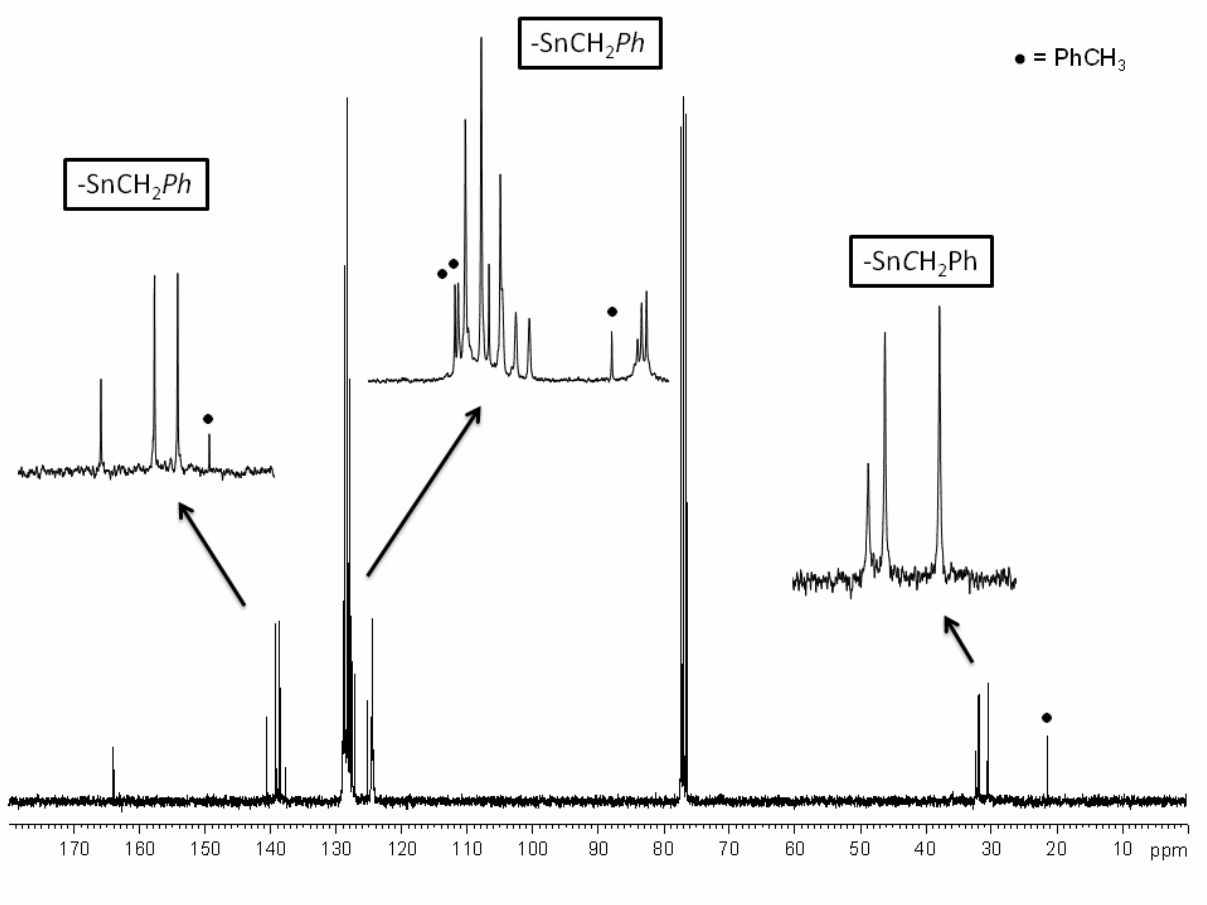

Fig. S2. $^{13}C\{^{1}H\}$ NMR Spectrum of **2** ($CDCl_3$, 200 K, 75.467 MHz)

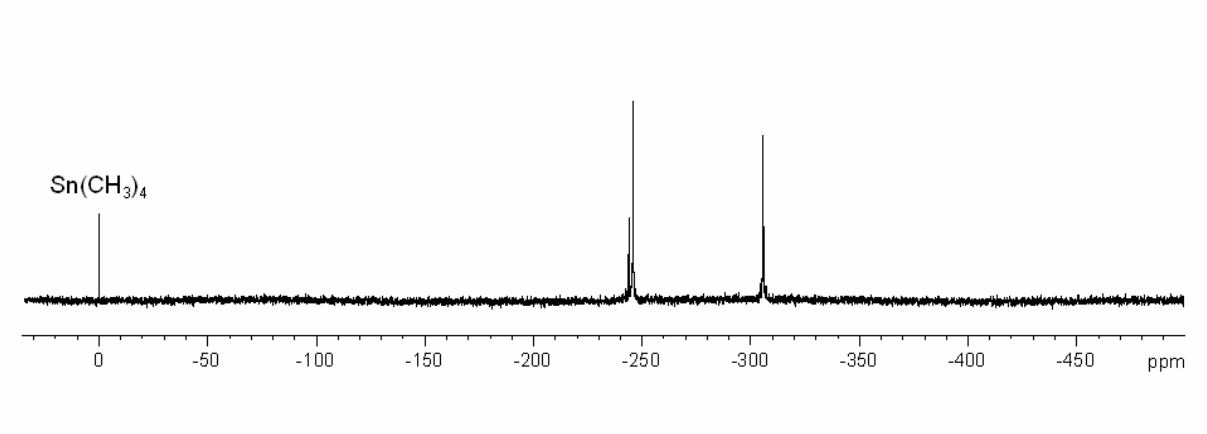

Fig. S3. $^{119}Sn\{^{1}H\}$ NMR Spectrum of **2** ($CDCl_3$, 297 K, 111.920 MHz)

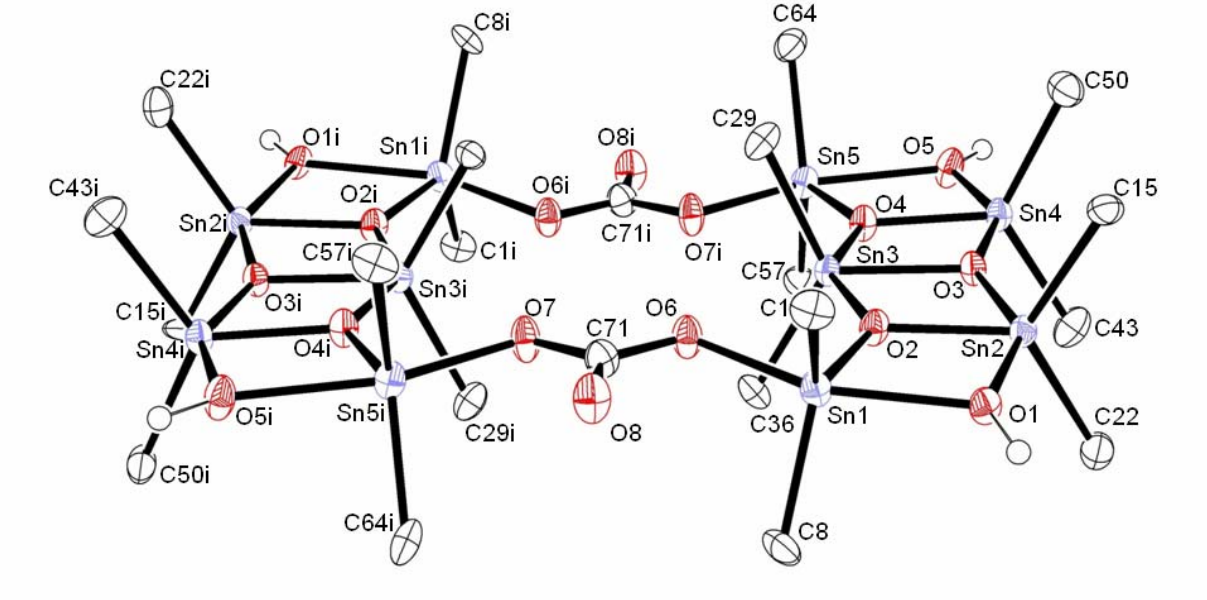

Fig. S4. ORTEP view of the molecular structure of $((PhCH_2)_2SnO)_6[((PhCH_2)_2SnOH)_2(CO_3)]_2$ (**2**) with crystallographic numbering scheme (hydrogen atoms, except for OH groups, are omitted for clarity, and only the methylene carbon atoms of the benzyl ligands linked to the tin centres are shown; Sn blue, O red, C white).

Table S1. Selected bond lengths (Å) and angles (deg) for **2**.

Sn–C		*Sn–μ-OH*		*Sn–μ$_3$-O*	
Sn(1)-C(1)	2.132(4)	Sn(1)-O(1)	2.233(3)	Sn(1)-O(2)	2.016(3)
Sn(1)-C(8)	2.145(4)	Sn(2)-O(1)	2.143(3)	Sn(2)-O(2)	2.029(3)
Sn(2)-C(15)	2.138(4)	Sn(2)-O(1)	2.143(3)	Sn(2)-O(3)	2.126(3)
Sn(2)-C(22)	2.153(4)	Sn(4)-O(5)	2.144(3)	Sn(3)-O(2)	2.126(3)
Sn(3)-C(29)	2.142(4)	Sn(5)-O(5)	2.257(3)	Sn(3)-O(3)	2.070(2)
Sn(3)-C(36)	2.138(4)			Sn(3)-O(4)	2.136(3)
Sn(4)-C(43)	2.151(4)	*–OC(O)O–*		Sn(4)-O(3)	2.127(3)
Sn(4)-C(50)	2.155(4)	O(6)-C(71)	1.297(5)	Sn(4)-O(4)	2.012(3)
Sn(5)-C(57)	2.133(4)	O(7)-C(71)	1.308(5)	Sn(5)-O(4)	2.025(3)
Sn(5)-C(64)	2.141(4)	O(8)-C(71)	1.256(5)		
				Sn–μ-CO$_3$	
				Sn(1)-O(6)	2.115(3)
				Sn(5)-O(7^{i})	2.118(3)

Sn(1)-O(2)-Sn(2)	114.20(12)	O(1)-Sn(2)-C(22)	97.15(14)
Sn(1)-O(2)-Sn(3)	139.27(13)	O(2)-Sn(2)-C(15)	117.06(14)
Sn(2)-O(1)-Sn(1)	101.79(11)	O(3)-Sn(2)-C(15)	100.93(13)
Sn(2)-O(2)-Sn(3)	106.36(11)	O(3)-Sn(2)-C(22)	96.95(14)
Sn(2)-O(3)-Sn(4)	150.91(13)	C(15)-Sn(2)-O(1)	96.78(13)
Sn(3)-O(3)-Sn(2)	104.88(11)	C(15)-Sn(2)-O(1)	96.78(13)
Sn(3)-O(3)-Sn(4)	104.11(11)	C(15)-Sn(2)-C(22)	120.86(16)
Sn(4)-O(4)-Sn(3)	105.86(11)	O(2)-Sn(2)-C(22)	121.98(14)
Sn(4)-O(4)-Sn(5)	114.30(12)	O(2)-Sn(2)-O(3)	74.74(10)
Sn(4)-O(5)-Sn(5)	100.78(11)	O(3)-Sn(2)-O(1)	147.36(10)
Sn(5)-O(4)-Sn(3)	139.71(13)	O(2)-Sn(3)-C(29)	100.05(13)
O(2)-Sn(1)-C(1)	122.60(14)	O(2)-Sn(3)-C(36)	95.70(14)
O(2)-Sn(1)-C(8)	116.32(15)	O(3)-Sn(3)-C(29)	114.98(14)
O(6)-Sn(1)-C(1)	103.86(14)	O(3)-Sn(3)-C(36)	120.23(13)
O(6)-Sn(1)-C(8)	97.02(15)	O(4)-Sn(3)-C(29)	95.76(14)
O(2)-Sn(1)-O(1)	71.14(10)	O(4)-Sn(3)-C(36)	97.76(13)
O(6)-Sn(1)-O(1)	150.20(10)	C(36)-Sn(3)-C(29)	124.78(16)
C(8)-Sn(1)-O(1)	96.61(14)	O(2)-Sn(3)-O(4)	148.07(10)
O(2)-Sn(1)-O(6)	79.07(10)	O(3)-Sn(3)-O(2)	73.93(10)
O(1)-Sn(1)-C(1)	91.94(14)	O(3)-Sn(3)-O(4)	74.27(10)
C(1)-Sn(1)-C(8)	119.98(18)	O(6)-C(71)-O(7)	115.7(4)
C(71)-O(6)-Sn(1)	114.9(3)	O(8)-C(71)-O(6)	123.0(4)
		O(8)-C(71)-O(7)	121.3(4)

Symmetry transformations used to generate equivalent atoms: i = -*x*+2,-*y*+1,-*z*+1.

Table S2. Selected bond lengths (Å) and angles (deg) for **3**.

Sn–C		*Sn–μ_4-O*			
Sn(1)-C(1)	2.132(8)	Sn(2)-O(4)	2.121(5)	Sn(3)-O(3)	2.120(5)
Sn(2)-C(8)	2.142(7)	Sn(3)-O(4)	2.306(5)	Sn(3)-O(7)	2.065(5)
Sn(3)-C(15)	2.127(7)	Sn(4)-O(4)	2.130(5)	Sn(3)-O(8)	2.077(5)
Sn(4)-C(22)	2.143(8)	Sn(5)-O(4)	2.221(5)	Sn(3)-O(9)	2.063(5)
Sn(5)-C(29)	2.144(8)			Sn(4)-O(9)	2.104(5)
Sn(6)-C(36)	2.130(7)	*Sn–μ-OH*		Sn(4)-O(10)	2.100(5)
		Sn(1)-O(1)	2.049(5)	Sn(4)-O(11)	2.109(5)
Sn–OH_2		Sn(1)-O(2)	2.065(5)	Sn(5)-O(6)	2.044(5)
Sn(1)-O(15)	2.182(6)	Sn(1)-O(3)	2.053(5)	Sn(5)-O(8)	2.096(5)
Sn(1)-O(16)	2.209(5)	Sn(2)-O(2)	2.104(5)	Sn(5)-O(11)	2.081(5)
Sn(6)-O(13)	2.171(5)	Sn(2)-O(5)	2.107(5)	Sn(5)-O(12)	2.127(3)
Sn(6)-O(14)	2.168(6)	Sn(2)-O(6)	2.079(5)	Sn(6)-O(5)	2.059(4)
		Sn(2)-O(7)	2.120(5)	Sn(6)-O(10)	2.072(5)
				Sn(6)-O(12)	2.048(3)

O(1)-Sn(1)-O(2)	90.0(2)	O(9)-Sn(3)-O(7)	143.9(2)
O(1)-Sn(1)-O(3)	84.3(2)	O(9)-Sn(3)-O(8)	89.2(2)
O(3)-Sn(1)-O(2)	90.6(2)	O(7)-Sn(3)-O(8)	94.7(2)
O(3)-Sn(1)-C(1)	99.9(3)	O(9)-Sn(3)-O(3)	81.1(2)
O(1)-Sn(1)-O(15)	83.1(2)	O(7)-Sn(3)-O(3)	83.8(2)
O(2)-Sn(1)-O(15)	86.5(2)	O(8)-Sn(3)-O(3)	160.8(2)
O(1)-Sn(1)-O(16)	79.1(2)	O(9)-Sn(3)-C(15)	110.4(3)
O(2)-Sn(1)-O(16)	167.0(2)	O(7)-Sn(3)-C(15)	104.1(2)
O(15)-Sn(1)-O(16)	85.2(2)	O(8)-Sn(3)-C(15)	100.5(3)
O(1)-Sn(1)-C(1)	165.7(3)	O(3)-Sn(3)-C(15)	98.5(3)
O(2)-Sn(1)-C(1)	103.6(3)	O(9)-Sn(3)-O(4)	74.68(18)
O(3)-Sn(1)-O(15)	167.0(2)	O(7)-Sn(3)-O(4)	72.49(17)
O(3)-Sn(1)-O(16)	95.2(2)	O(8)-Sn(3)-O(4)	72.1(2)
C(1)-Sn(1)-O(15)	93.1(3)	O(3)-Sn(3)-O(4)	89.31(19)
C(1)-Sn(1)-O(16)	86.8(3)	C(15)-Sn(3)-O(4)	171.2(3)
O(6)-Sn(2)-O(2)	161.3(2)	Sn(1)-O(1)-Sn(4)	137.5(3)
O(2)-Sn(2)-O(5)	87.9(2)	Sn(1)-O(2)-Sn(2)	139.0(3)
O(6)-Sn(2)-O(7)	86.1(2)	Sn(1)-O(3)-Sn(3)	136.4(3)
O(2)-Sn(2)-O(7)	87.4(2)	Sn(2)-O(4)-Sn(3)	101.61(18)
O(5)-Sn(2)-O(7)	161.35(19)	Sn(2)-O(4)-Sn(4)	145.4(3)
O(6)-Sn(2)-O(4)	75.2(2)	Sn(2)-O(4)-Sn(5)	100.8(2)
O(2)-Sn(2)-O(4)	86.2(2)	Sn(3)-O(7)-Sn(2)	110.2(2)
O(5)-Sn(2)-O(4)	86.35(19)	Sn(3)-O(8)-Sn(5)	113.5(2)
O(7)-Sn(2)-O(4)	75.33(18)	Sn(3)-O(9)-Sn(4)	107.7(2)
O(6)-Sn(2)-C(8)	100.6(3)	Sn(4)-O(4)-Sn(3)	98.63(19)
O(2)-Sn(2)-C(8)	97.7(3)	Sn(4)-O(4)-Sn(5)	102.50(19)
O(5)-Sn(2)-C(8)	100.1(3)	Sn(5)-O(4)-Sn(3)	100.9(2)
O(7)-Sn(2)-C(8)	98.4(3)	Sn(5)-O(6)-Sn(2)	108.5(2)
O(4)-Sn(2)-C(8)	172.6(3)	Sn(6)-O(5)-Sn(2)	138.2(3)
O(6)-Sn(2)-O(5)	92.6(2)		

Table S3. Selected bond lengths (Å) and angles (deg) for **4**.

Sn–C		*Sn–μ-OH*			
Sn(2)-C(1)	2.146(11)	Sn(1)-O(2)	2.037(8)	Sn(5)-O(6)	2.072(7)
Sn(3)-C(8)	2.137(10)	Sn(1)-O(3)	2.050(6)	Sn(5)-O(11)	2.061(7)
Sn(4)-C(15)	2.130(10)	Sn(1)-O(1)	2.047(7)	Sn(5)-O(8)	2.096(6)
Sn(5)-C(22)	2.140(10)	Sn(2)-O(2)	2.122(7)	Sn(5)-O(12)	2.119(6)
Sn(6)-C(29)	2.152(9)	Sn(2)-O(5)	2.127(6)	Sn(6)-O(5)	2.040(6)
		Sn(2)-O(6)	2.100(6)	Sn(6)-O(10)	2.075(7)
Sn–μ₄-O		Sn(2)-O(7)	2.106(7)	Sn(6)-O(12)	2.072(6)
Sn(2)-O(4)	2.119(7)	Sn(3)-O(3)	2.161(7)		
Sn(3)-O(4)	2.292(6)	Sn(3)-O(7)	2.066(7)	*Sn–η-OTf*	
Sn(4)-O(4)	2.156(7)	Sn(3)-O(8)	2.068(7)	Sn(6)-O(14)	2.229(7)
Sn(5)-O(4)	2.239(6)	Sn(3)-O(9)	2.070(7)		
		Sn(4)-O(1)	2.116(7)	*F_3CS–O*	
Sn–OH_2		Sn(4)-O(9)	2.114(6)	S(1)-O(14)	1.450(7)
Sn(6)-O(13)	2.198(7)	Sn(4)-O(10)	2.082(6)	S(1)-O(15)	1.409(8)
		Sn(4)-O(11)	2.097(6)	S(1)-O(16)	1.427(9)

$O(2^i)$-Sn(1)-O(2)	180.000(2)	O(5)-Sn(6)-C(29)	166.8(3)
$O(2^i)$-Sn(1)-$O(1^i)$	91.9(3)	O(5)-Sn(6)-O(13)	80.9(3)
O(2)-Sn(1)-$O(1^i)$	88.9(3)	O(5)-Sn(6)-O(14)	83.3(3)
O(1)-Sn(1)-$O(3^i)$	91.1(3)	O(12)-Sn(6)-O(10)	88.7(3)
O(3)-Sn(1)-$O(3^i)$	180.000(2)	O(12)-Sn(6)-C(29)	102.4(3)
O(6)-Sn(2)-O(7)	84.9(3)	O(12)-Sn(6)-O(13)	165.8(3)
O(2)-Sn(2)-C(1)	96.8(4)	O(12)-Sn(6)-O(14)	93.7(3)
O(5)-Sn(2)-C(1)	98.9(4)	O(10)-Sn(6)-C(29)	101.8(3)
Sn(1)-O(1)-Sn(4)	138.5(4)	O(10)-Sn(6)-O(13)	85.8(3)
Sn(1)-O(2)-Sn(2)	137.8(4)	O(10)-Sn(6)-O(14)	171.3(3)
Sn(1)-O(3)-Sn(3)	134.1(3)	O(13)-Sn(6)-O(14)	90.0(3)
Sn(2)-O(4)-Sn(4)	145.8(3)	C(29)-Sn(6)-O(14)	85.9(3)
Sn(2)-O(4)-Sn(5)	101.0(3)	C(29)-Sn(6)-O(13)	91.6(4)
Sn(2)-O(4)-Sn(3)	101.1(2)	S(1)-O(14)-Sn(6)	144.4(4)
Sn(3)-O(7)-Sn(2)	109.5(3)	O(14)-S(1)-C(36)	100.2(6)
Sn(6)-O(5)-Sn(2)	138.9(3)	O(15)-S(1)-O(14)	112.3(4)
Sn(5)-O(6)-Sn(2)	107.4(3)	O(15)-S(1)-O(16)	114.5(5)
Sn(6)-O(12)-Sn(5)	136.1(3)	O(15)-S(1)-C(36)	108.5(7)
O(5)-Sn(6)-O(12)	85.9(3)	O(16)-S(1)-O(14)	115.3(5)
O(5)-Sn(6)-O(10)	88.6(3)	O(16)-S(1)-C(36)	104.4(7)

Symmetry transformations used to generate equivalent atoms: i = -*x*+1,-*y*+1,-*z*+1